

A discontinuous Galerkin method for wave propagation in coupled elastic-acoustic media

Kaihang Guo¹, Sebastian Acosta², Jesse Chan¹

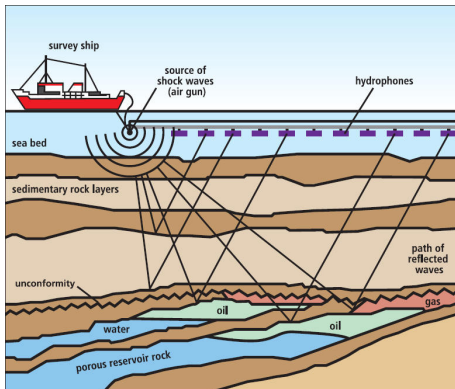
¹Department of Computational and Applied Mathematics, Rice University

²Department of Pediatrics-Cardiology, Baylor College of Medicine

SIAM LA-TX Sectional Conference
Nov 1-3, 2019

Motivation

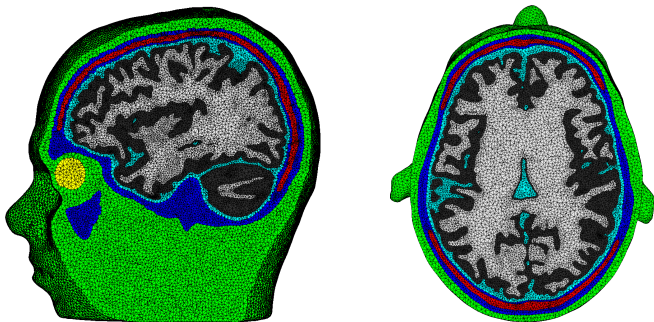
In marine seismology, waves propagate through different subsurface layers, resulting in models with fluid-solid interfaces.



Marine seismic exploration

Motivation

In photoacoustic tomography (PAT), researchers want to locate brain tumors through reconstruction of initial pressure condition.



FEM mesh of an adult head

Outline

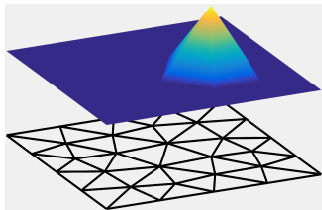
- Elastic-acoustic coupled DG
- Numerical experiments
- Application examples

- Elastic-acoustic coupled DG
- Numerical experiments
- Application examples

Finite element methods

Finite element methods (FEM):

- Unstructured meshes.
- Continuous piecewise polynomial approximation.
- Continuous PDE (example: advection)



$$\frac{\partial u}{\partial t} = \frac{\partial u}{\partial x}$$

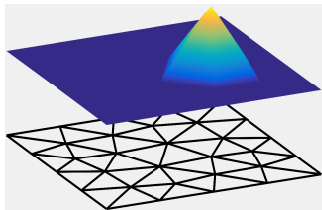
- FEM weak form over domain Ω

$$\int_{\Omega} \frac{\partial u}{\partial t} \phi = \int_{\Omega} \frac{\partial u}{\partial x} \phi, \quad u, \phi \in V_h$$

Finite element methods

Finite element methods (FEM):

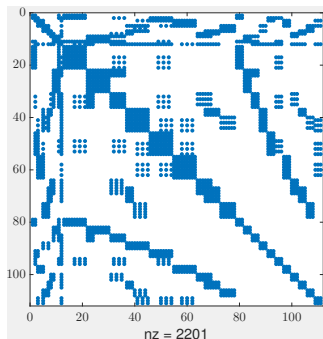
- Unstructured meshes.
- Continuous piecewise polynomial approximation.



FEM yields system of ODEs with global mass matrix \mathbf{M}_Ω , discretization matrix \mathbf{A} .

$$\mathbf{M}_\Omega \frac{d\mathbf{u}}{dt} = \mathbf{A}\mathbf{u}.$$

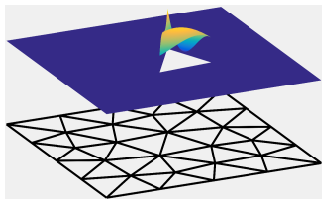
FEM mass matrix is globally coupled.



Basics of discontinuous Galerkin methods

Discontinuous Galerkin (DG) methods:

- Unstructured meshes.
- Weak continuity across faces.
- Continuous PDE (example: advection)



$$\frac{\partial u}{\partial t} = \frac{\partial f(u)}{\partial x}, \quad f(u) = u.$$

- Local DG form with numerical flux \mathbf{f}^* : find $u \in P^N(D^k)$ such that

$$\int_{D_k} \frac{\partial u}{\partial t} \phi = \int_{D_k} \frac{\partial f(u)}{\partial x} \phi + \int_{\partial D_k} \mathbf{n} \cdot (\mathbf{f}^* - \mathbf{f}(u)) \phi, \quad \forall \phi \in P^N(D^k).$$

Basics of discontinuous Galerkin methods

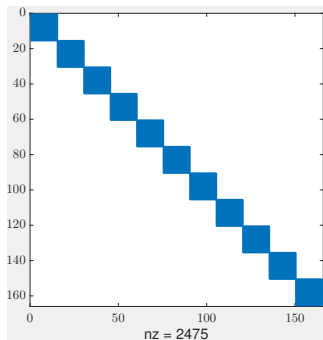
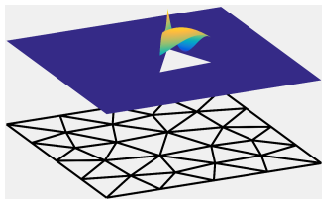
Discontinuous Galerkin (DG) methods:

- Unstructured meshes.
- Weak continuity across faces.

DG in space yields system of ODEs

$$\mathbf{M}_{\Omega} \frac{d\mathbf{u}}{dt} = \mathbf{A}\mathbf{u}.$$

DG mass matrix decouples across elements,
inter-element coupling only through \mathbf{A} .



Global mass matrix \mathbf{M}_{Ω} .

High order DG methods

- Unstructured (tetrahedral) meshes for geometric flexibility.
- High order: low numerical dissipation and dispersion.
- High order approximations: more accurate per unknown.
- Explicit time stepping: high performance on many-core.

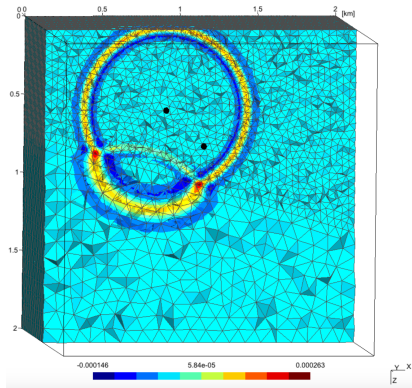
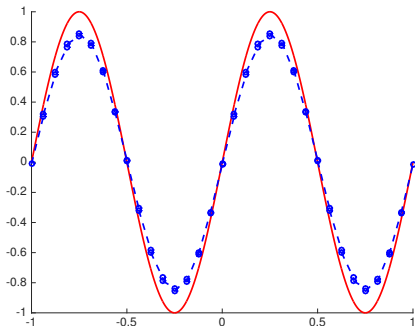


Figure courtesy of Axel Modave.

High order DG methods

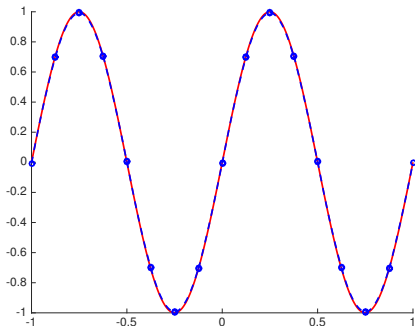
- Unstructured (tetrahedral) meshes for geometric flexibility.
- High order: low numerical dissipation and dispersion.
- High order approximations: more accurate per unknown.
- Explicit time stepping: high performance on many-core.



Fine linear approximation.

High order DG methods

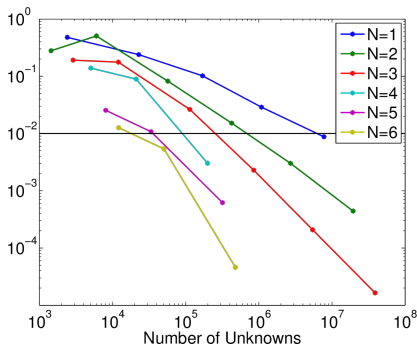
- Unstructured (tetrahedral) meshes for geometric flexibility.
- High order: low numerical dissipation and dispersion.
- High order approximations: more accurate per unknown.
- Explicit time stepping: high performance on many-core.



Coarse quadratic approximation.

High order DG methods

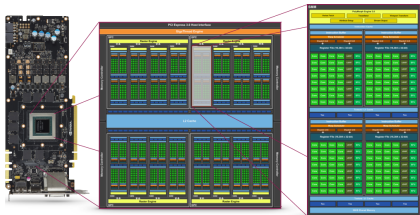
- Unstructured (tetrahedral) meshes for geometric flexibility.
- High order: low numerical dissipation and dispersion.
- High order approximations: more accurate per unknown.
- Explicit time stepping: high performance on many-core.



Max errors vs. dofs.

High order DG methods

- Unstructured (tetrahedral) meshes for geometric flexibility.
- High order: low numerical dissipation and dispersion.
- High order approximations: more accurate per unknown.
- Explicit time stepping: high performance on many-core.



Graphics processing units (GPU).

Previous work

- Wilcox et al. constructed a DG-SEM scheme on quadrilateral and hexahedral meshes using Gauss-Lobatto quadrature by deriving an upwind numerical flux from the exact Riemann problem.¹
- Zhan et al. extended this approach to anisotropic elastic-acoustic media by solving a simplified Riemann problem on each inter-element interface.²
- Ye et al. circumvent the Riemann problem altogether by using a DG formulation with a dissipative upwind-like “penalty” flux.³

Wilcox, Stadler, Burstedde, Ghattas. 2010. A high-order discontinuous Galerkin method for wave propagation through coupled elastic-acoustic media.

Zhan, Ren, Zhuang, Sun, Liu. 2018. An exact Riemann solver for wave propagation in arbitrary anisotropic elastic media with fluid coupling.

Ye, de Hoop, Petrovitch, Pyrak-Nolte, Wilcox. 2016. A discontinuous Galerkin method with a modified penalty flux for the propagation and scattering of acousto-elastic waves.

First-order wave equations

- Acoustic wave equation:

$$\frac{1}{c^2} \frac{\partial p}{\partial t} = \nabla \cdot \mathbf{u}, \quad \frac{\partial \mathbf{u}}{\partial t} = \nabla p \quad (\text{fluid})$$

- Elastic wave equation:

$$\rho \frac{\partial \mathbf{v}}{\partial t} = \sum_{i=1}^d \mathbf{A}_i^T \frac{\partial \boldsymbol{\sigma}}{\partial \mathbf{x}_i}, \quad \mathbf{C}^{-1} \frac{\partial \boldsymbol{\sigma}}{\partial t} = \sum_{i=1}^d \mathbf{A}_i \frac{\partial \mathbf{v}}{\partial \mathbf{x}_i} \quad (\text{solid})$$

- Numerical scheme: high order, explicit time-stepping, parallelizable

Strong DG formulation

- Pure acoustic domain:

$$\begin{aligned}\left(\frac{1}{c^2} \frac{\partial p}{\partial t}, q\right)_{L^2(D^k)} &= (\nabla \cdot \mathbf{u}, q)_{L^2(D^k)} + \sum_{f \in \partial D^k \cap \Gamma_{aa}} \left\langle \frac{1}{2} \mathbf{n}^T [\![\mathbf{u}]\!] + \frac{\tau_p}{2} [\![p]\!], q \right\rangle_{L^2(f)} \\ \left(\frac{\partial \mathbf{u}}{\partial t}, \mathbf{w}\right)_{L^2(D^k)} &= (\nabla p, \mathbf{w})_{L^2(D^k)} + \sum_{f \in \partial D^k \cap \Gamma_{aa}} \left\langle \frac{1}{2} \mathbf{n}^T [p] + \frac{\tau_u}{2} [\![\mathbf{u}]\!], \mathbf{w} \right\rangle_{L^2(f)}\end{aligned}$$

- Pure elastic domain:

$$\begin{aligned}\left(\rho \frac{\partial \mathbf{v}}{\partial t}, \mathbf{w}\right)_{L^2(D^k)} &= \left(\sum_{i=1}^d \mathbf{A}_i^T \frac{\partial \boldsymbol{\sigma}}{\partial \mathbf{x}_i}, \mathbf{w}\right)_{L^2(D^k)} + \sum_{f \in \partial D^k \cap \Gamma_{ee}} \left\langle \frac{1}{2} \mathbf{A}_n^T [\![\boldsymbol{\sigma}]\!] + \frac{\tau_v}{2} \mathbf{A}_n^T \mathbf{A}_n [\![\mathbf{v}]\!], \mathbf{w} \right\rangle_{L^2(f)} \\ \left(\mathbf{C}^{-1} \frac{\partial \boldsymbol{\sigma}}{\partial t}, \mathbf{q}\right)_{L^2(D^k)} &= \left(\sum_{i=1}^d \mathbf{A}_i \frac{\partial \mathbf{v}}{\partial \mathbf{x}_i}, \mathbf{q}\right)_{L^2(D^k)} + \sum_{f \in \partial D^k \cap \Gamma_{ee}} \left\langle \frac{1}{2} \mathbf{A}_n [\![\mathbf{v}]\!] + \frac{\tau_\sigma}{2} \mathbf{A}_n \mathbf{A}_n^T [\![\boldsymbol{\sigma}]\!], \mathbf{q} \right\rangle_{L^2(f)}\end{aligned}$$

Γ_{aa} : acoustic-acoustic interfaces

Γ_{ee} : elastic-elastic interfaces

Weight-adjusted DG: stable, accurate, non-invasive

- High order wavespeeds: weighted mass matrices. Stable, but requires pre-computation/storage of inverses or factorizations!

$$\mathbf{M}_{1/c^2} \frac{d\mathbf{p}}{dt} = \mathbf{A}_h \mathbf{U}, \quad (\mathbf{M}_{1/c^2})_{ij} = \int_{D^k} \frac{1}{c^2(\mathbf{x})} \phi_j(\mathbf{x}) \phi_i(\mathbf{x}).$$

- **Weight-adjusted DG (WADG)**: energy stable approx. of \mathbf{M}_{1/c^2}

$$\mathbf{M}_{1/c^2} \approx \mathbf{M} (\mathbf{M}_{c^2})^{-1} \mathbf{M} \Rightarrow \frac{d\mathbf{p}}{dt} = \mathbf{M}^{-1} (\mathbf{M}_{c^2}) \mathbf{M}^{-1} \mathbf{A}_h \mathbf{U}$$

- Low storage matrix-free application of $\mathbf{M}^{-1} \mathbf{M}_{c^2}$ using **quadrature**-based interpolation and L^2 projection matrices $\mathbf{V}_q, \mathbf{P}_q$.

$$(\mathbf{M})^{-1} \mathbf{M}_{c^2} \text{RHS} = \underbrace{\mathbf{M}^{-1} \mathbf{V}_q^T \mathbf{W}}_{\mathbf{P}_q} \text{diag}(c^2) \mathbf{V}_q (\text{RHS}).$$

Energy stable elastic-acoustic coupling

- Typical DG approach: upwind flux (exact Riemann solver).
- Riemann problem is expensive and difficult to solve exactly in **heterogeneous** and **anisotropic** media.
- The numerical flux should be consistent with continuity conditions on elastic-acoustic interfaces

$$\mathbf{u} \cdot \mathbf{n} = \mathbf{v} \cdot \mathbf{n}, \quad \mathbf{A}_n^T \boldsymbol{\sigma} = p \mathbf{n}.$$

- Penalty term with parameter $\tau \geq 0$ adds upwind-like dissipation.
- Our goal is to find a numerical flux such that the DG scheme is energy stable.

Energy stable elastic-acoustic coupling

(Elastic)

$$\begin{aligned} \frac{1}{2} \langle pn - A_n^T \sigma - (I - nn^T) A_n^T \sigma, w \rangle + \frac{\tau}{2} \langle (u - v) \cdot n, w \cdot n \rangle \\ \frac{1}{2} \langle (u - v) \cdot n, A_n^T q \rangle + \frac{\tau}{2} \langle (pn - A_n^T \sigma), A_n^T q \rangle \end{aligned}$$



$$\begin{aligned} u \cdot n &= v \cdot n \\ A_n^T \sigma &= pn \end{aligned}$$

$$\begin{aligned} \frac{1}{2} \langle (A_n^T \sigma - pn) \cdot n, w \cdot n \rangle + \frac{\tau}{2} \langle (v - u) \cdot n, w \cdot n \rangle \\ \frac{1}{2} \langle (v - u) \cdot n, q \rangle + \frac{\tau}{2} \langle (A_n^T \sigma - pn) \cdot n, q \rangle \end{aligned}$$

(Acoustic)

Theoretical results

Theorem (Consistency)

The coupled discontinuous Galerkin scheme is consistent.

Theorem (Energy stability)

The coupled discontinuous Galerkin scheme is energy stable for $\tau_u = \tau_v \geq 0, \tau_p = \tau_\sigma \geq 0$, in the sense that

$$\begin{aligned} & \sum_{D^k \in \Omega_h^e} \frac{\partial}{\partial t} \left((\rho \mathbf{v}, \mathbf{v})_{L^2(D^k)} + (\mathbf{C}^{-1} \boldsymbol{\sigma}, \boldsymbol{\sigma})_{L^2(D^k)} \right) + \sum_{D^k \in \Omega_h^a} \frac{\partial}{\partial t} \left(\left(\frac{p}{c^2}, p \right)_{L^2(D^k)} + (\mathbf{u}, \mathbf{u})_{L^2(D^k)} \right) \\ &= - \sum_{f \in \Gamma_{aa}} \int_f \left(\tau_p \llbracket p \rrbracket^2 + \tau_u (\mathbf{n} \cdot \llbracket \mathbf{u} \rrbracket)^2 \right) - \sum_{f \in \Gamma_{ee}} \int_f \left(\frac{\tau_u}{2} |\mathbf{A}_n \llbracket \mathbf{v} \rrbracket|^2 + \frac{\tau_p}{2} |\mathbf{A}_n^T \llbracket \boldsymbol{\sigma} \rrbracket|^2 \right) \\ & \quad - \sum_{f \in \Gamma_{ea} \cup \Gamma_{ae}} \int_f \left(\frac{\tau_u}{2} |\mathbf{n}^T (\mathbf{u} - \mathbf{v})|^2 + \frac{\tau_p}{2} |\rho \mathbf{n} - \mathbf{A}_n^T \boldsymbol{\sigma}|^2 \right) \leq 0, \end{aligned}$$

where Ω_h^a and Ω_h^e denote the acoustic and elastic computational domain, respectively.

Outline

- Elastic-acoustic coupled DG
- Numerical experiments
- Application examples

Spectra and choice of penalty parameter

Let \mathbf{L} denote the matrix induced by the global semi-discrete DG formulation, such that the time evolution of the global solution is governed by

$$\frac{\partial \mathbf{Q}}{\partial t} = \mathbf{L} \mathbf{Q}$$

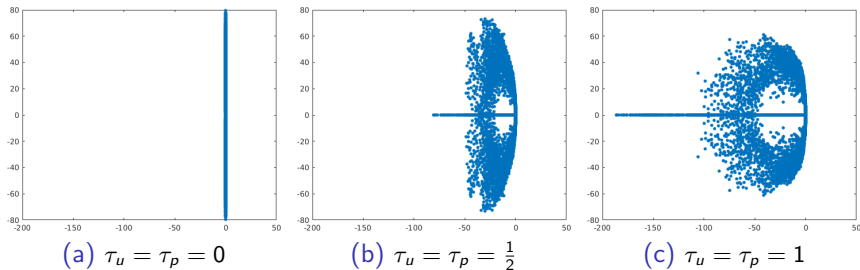
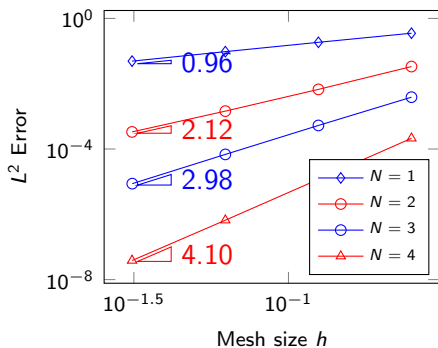
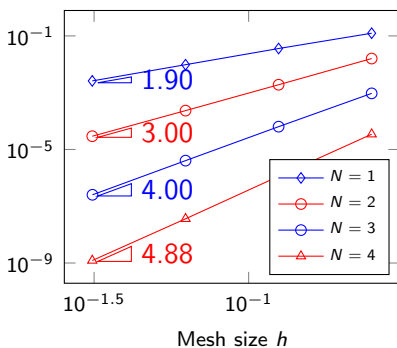


Figure: Spectra for $N = 3$ on a non-curved uniform mesh with $h = 1/4$. For all cases, the largest real part of the spectra is $O(10^{-14})$.

Classical interface problems: Scholte wave



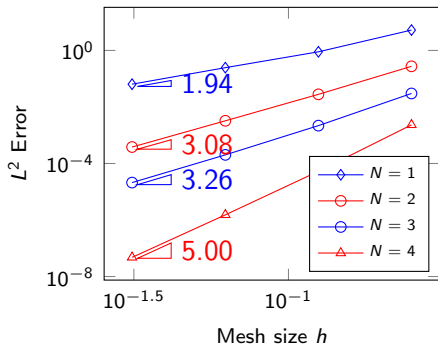
(a) Central flux ($\tau_u = \tau_p = 0$)



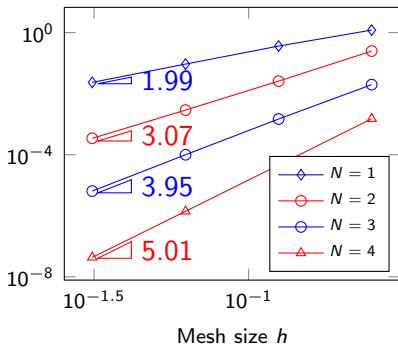
(b) Penalty flux ($\tau_u = \tau_p = 1$)

Figure: Convergence of L^2 errors for the Scholte wave solution

Classical interface problems: Snell's law



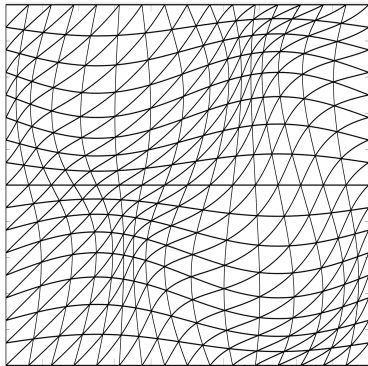
(a) Central flux ($\tau_u = \tau_p = 0$)



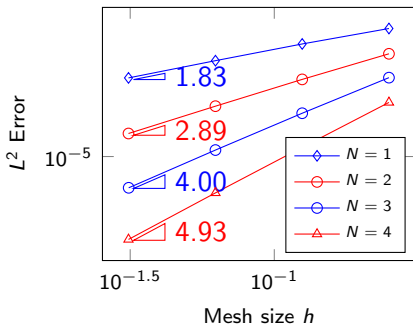
(b) Penalty flux ($\tau_u = \tau_p = 1$)

Figure: Convergence of L^2 errors for the Snell's law solution

Extension to curvilinear meshes



(a) Curvilinear mesh



(b) Scholte wave (curvilinear)

Extension to curvilinear meshes

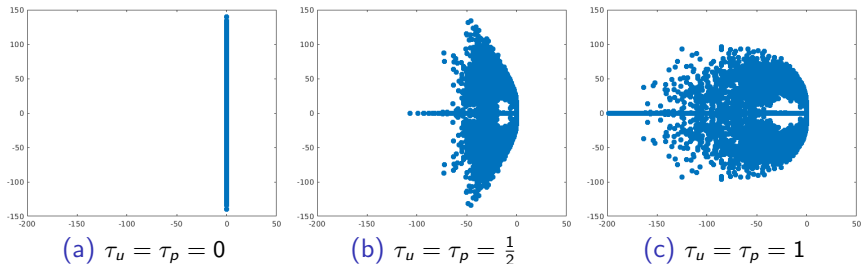


Figure: Spectra of the discontinuous Galerkin discretization matrix for central and penalty fluxes on a warped curvilinear mesh of degree $N = 3$. For all cases, the largest real part of the spectra is $O(10^{-14})$.

Outline

- Elastic-acoustic coupled DG
- Numerical experiments
- Application examples

Homogeneous anisotropic media

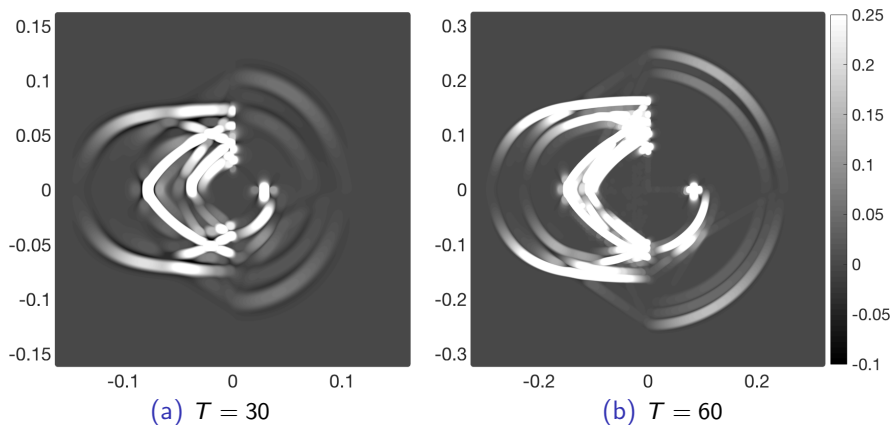


Figure: An example of wave propagation in homogeneous anisotropic-isotropic acoustic-elastic media.

Heterogeneous anisotropic media

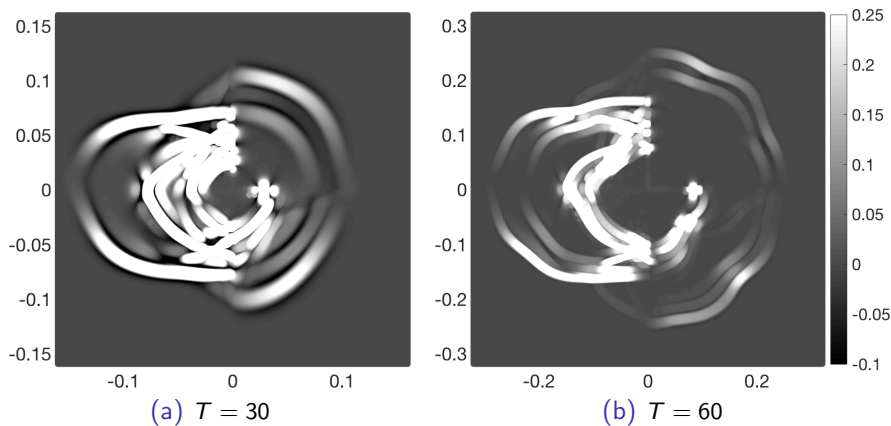
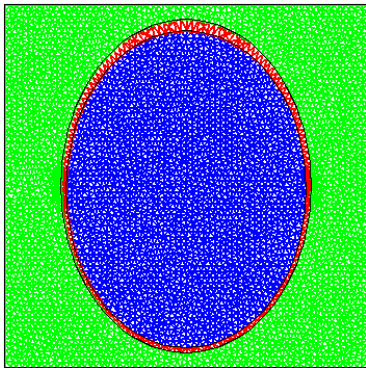
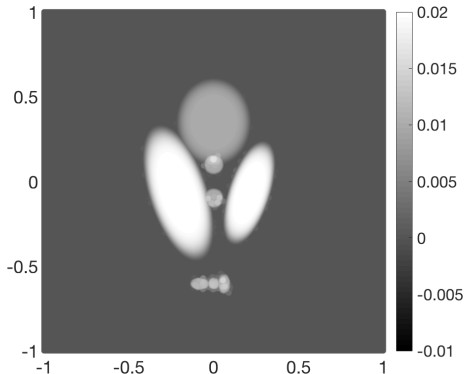


Figure: An example of wave propagation in heterogeneous anisotropic-isotropic acoustic-elastic media.

Photoacoustic tomography (PAT)

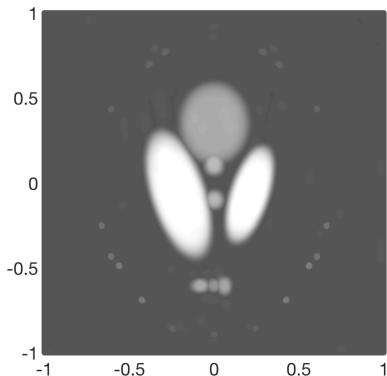


(a) Mesh

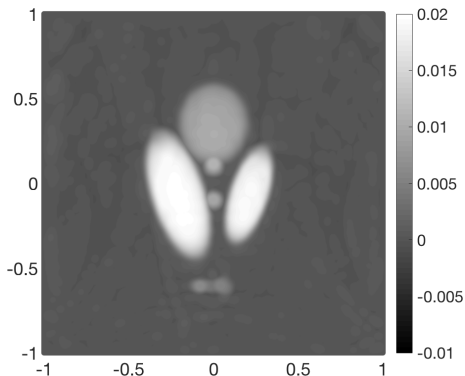


(b) Exact initial pressure

Photoacoustic tomography (PAT)



(a) Reconstruction after 5 iterations

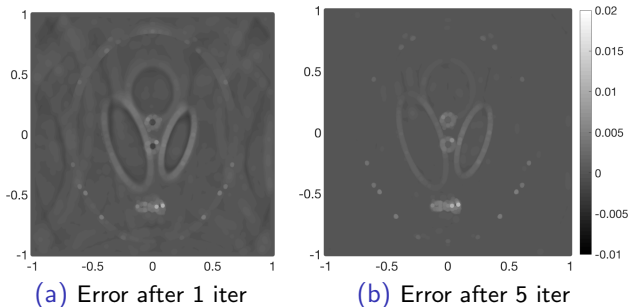


(b) Purely acoustic reconstruction

Photoacoustic tomography (PAT)

Iteration	Fine	Fine (acous)	Coarse	Coarse (acous)
1	0.140530	0.147435	0.140556	0.147103
2	0.094658	0.133881	0.094811	0.133508
3	0.075081	0.130397	0.075347	0.130010
4	0.065585	0.129331	0.065941	0.128939
5	0.060577	0.128973	0.060998	0.128577

Table: Relative L^2 errors at each iteration



Summary and acknowledgements

- We derive a numerical flux across elastic-acoustic interfaces with a very simple form.
- The proposed scheme can be applied on unstructured tetrahedral meshes and general curvilinear meshes.
- The resulting DG method is efficient, provably energy stable, and high order accurate for arbitrary heterogeneous and anisotropic media.

Thank you! Questions?



-
- Guo, Acosta, Chan. 2019. A weight-adjusted DG method for wave propagation in coupled elastic-acoustic media.
- Guo, Chan. 2018. Bernstein-Bezier weight-adjusted discontinuous Galerkin methods for wave propagation (JCP).
- Chan, Hewett, Warburton. 2016. Weight-adjusted DG methods: wave propagation in heterogeneous media (SISC).
- Chan. 2017. Weight-adjusted DG methods: matrix-valued weights and elastic wave prop. in heterogeneous media (IJNME).
- Chan, Warburton. 2015. GPU-accelerated Bernstein-Bezier discontinuous Galerkin methods for wave propagation (SISC).